

Chapter 5

Radiative Transfer and Line Formation

5.1 Column Density

Consider an arbitrary structure of gas with a number density $n(x, y, z)$. The quasar line of sight (LOS) will probe a finite distance through the cloud for a length L . At each infinitesimal location along the LOS, $l \rightarrow l + dl$, the gas density sampled, $n(l)$, will depend upon the xyz coordinate of $l = l(x, y, z)$; exactly how depends upon the parameterization of the structure geometry. The point is that the density may not be constant throughout the cloud. The column density, N , is defined as the integrated number density along the LOS, and is expressed

$$N = \int_0^L n(l) dl. \quad (5.1)$$

In practice, one has no knowledge of $n(x, y, z)$, the path length, L , nor of any idea of how to formulate a geometry of the gaseous structure. However, N is extractable directly from the absorption line data using the basic physics of bound-bound atomic transitions. From N , metallicities and ionization conditions of the gas can be inferred assuming that the ionization corrections can be made accurately. In the following sections, we will develop the formalism by which N is obtained from the absorption line data.

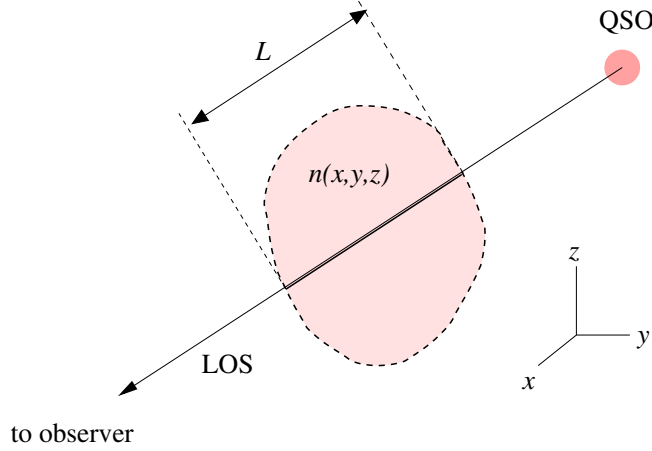


Figure 5.1: — A schematic of the geometry of the line of sight (LOS) intersection of an absorbing cloud. The LOS passes through the cloud in some arbitrary coordinate system, which if known, could be used to obtain the path length through the cloud and $n(l)$ from $n(x, y, z)$, the density profile of the cloud. In practice, no information is available and only the integral, Eq. 5.1, giving the column density, N , can be measured from the data.

5.2 Optical Depth

Consider a plane parallel slab of thickness L with depth coordinate $x = 0 \rightarrow L$, where the light incident on the slab at $x = 0$ is I_λ^o . The incremental extinction of light intensity dI_λ over an infinitesimal depth $x \rightarrow x + dx$ will be proportional to the intensity I_λ at x

$$dI_\lambda = -\kappa_\lambda \rho I_\lambda dx, \quad (5.2)$$

where κ_λ is the mass absorption coefficient [$\text{cm}^2 \text{g}^{-1}$], and $\rho(x)$ is the mass density [g cm^{-3}] of material in the slab. The two types of extinction described here are (1) bound-free absorption due to ionization, where an electron is kicked into the gas and is thermalized, and (2) scattering, where a photon direction is deviated and therefore removed from the solid angle of observation. We can rewrite Eq. 5.2 as

$$dI_\lambda = -I_\lambda d\tau_\lambda, \quad (5.3)$$

where

$$d\tau_\lambda = \kappa_\lambda \rho dx. \quad (5.4)$$

The total optical depth through the cloud

$$\tau_\lambda = \int_0^L \kappa_\lambda \rho dx \quad [\text{unitless}], \quad (5.5)$$

is the integrated extinction (i.e., optical depth) of I_λ emerging from the slab. Analogous to κ_λ is the line absorption coefficient ℓ_λ , which describes the absorption of photons by bound-bound atomic transitions. It is defined in the same manner as in Eq. 5.2,

$$dI_\lambda = -\ell_\lambda \rho I_\lambda dx, \quad (5.6)$$

$$d\tau_\lambda = -\ell_\lambda \rho dx, \quad (5.7)$$

but in this case it describes the absorption of photons by the *internal* excitation of atoms; the energy is not thermalized by introducing free electrons into the gas, as in ionization. However, when an electron deexcites, the process could mimic scattering (electron falls directly back to its original state sending a photon of identical energy out of the observed solid angle). It can also result in a redistribution of the photon energy field (electron cascades to less excited states before reaching its original state, sending a few to several photons of lesser energies into the gas).

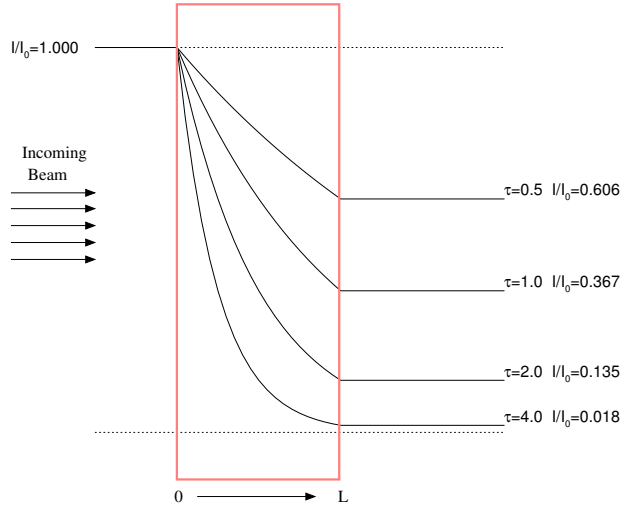


Figure 5.2: — A schematic of absorption through a cloud with path length, L , for $\tau = 0.5, 1.0, 2.0,$ and 4.0 . The incoming beam (from the left) is attenuated following Eq. 5.8. Since τ is the integral over L of $\kappa_\lambda \rho$, or $\ell_\lambda \rho$ for line opacity, the examples are for different opacities, cloud densities, or both.

The solution to Eqs. 5.2 and 5.6 is of the form

$$I_\lambda(x > L) = I_\lambda^o \exp[-\tau_\lambda], \quad (5.8)$$

where I_λ^o is the intensity of the light incident on the slab face at $x = 0$, I_λ is the intensity emerging from the cloud at L , and τ_λ is the integrated

optical depth either for extinction, via κ_λ or bound–bound line absorption via ℓ_λ . In Fig. 5.2. Eq. 5.8 is illustrated for various optical depths.

Equation 5.8 is the workhorse expression for analysis of quasar absorption line data. In the following sections, we will “derive” the detailed expression for $\tau_\lambda = \ell_\lambda \rho$ for bound–bound atomic transitions. From this expression, one can extract the column density and the details about the thermal and/or turbulent conditions of the gas.

5.3 Natural Broadening

We wish to motivate the functional form for the line absorption coefficient, ℓ_λ , which describes the *natural* line broadening mechanism due to the physics of bound–bound transitions.

Consider a photon incident upon an atom with a bound electron. For the following, we will present a classical treatment. A photon is an oscillating electric field. Let the direction of the field oscillation be $y(t)$ and the propagation direction of the photon be x . As the photon is incident upon the atom, the electron experiences an oscillation (in the y direction). In the classical world, the electron experiences an energy loss as it accelerates, and therefore radiates energy away, under the influence of the oscillating electric field. Thus, the electron experiences a force from its own radiation that damps the acceleration. This motivates the use of a damping term when describing the electron oscillatory motion. However, in a quantum mechanical treatment, the electron radiates only when it actually undergoes a bound–bound transition. Later, we will see that the damping term is related to the uncertainty in the energy levels.

The electron obeys the harmonic oscillator equation

$$\frac{d^2 y}{dt^2} + \Gamma \frac{dy}{dt} + \omega_o^2 y = \frac{e}{m_e} E_o \exp(i\omega t), \quad (5.9)$$

where e is the electron charge, m_e is the electron mass, Γ is the damping constant, $\omega = 2\pi c/\lambda$ is the incident photon (oscillation) frequency, and E_o is the amplitude of the electric field energy. The term ω_o is defined by the energy separation of the bound–bound transition via $E_u - E_l = hc/\lambda_o = 2\pi h\omega_o$, where E_u and E_l are the upper, u , and lower, l , energy levels, and h is Planck’s constant. The solution to Eq. 5.9 is

$$y(t) = \left(\frac{e}{m_e} \right) \frac{E(t)}{\omega_o^2 - \omega^2 + i\Gamma\omega}, \quad (5.10)$$

with $E(t) = E_o \exp(i\omega t)$. This describes the classical amplitude of dipole oscillation in a photon field. The solution is in resonance when $\omega = \omega_o$, i.e. the photon frequency matches the energy level difference.

Now, to obtain the degree of absorption, we must consider how a damped dipole oscillation attenuates the electric field. As the photon propagates in the x direction, the attenuation follows

$$E(x, t) = E_o \exp \left[i\omega \left\{ t - \frac{x}{c} \left(\frac{\epsilon}{\epsilon_o} \right)^{1/2} \right\} \right], \quad (5.11)$$

where the attenuation term is $(\epsilon/\epsilon_o)^{1/2} = c/v$, where ϵ is the permittivity due to the electron oscillation, ϵ_o is the permittivity of free space, and v is the photon velocity. If the column density of dipole oscillators is N (i.e., the column density of atoms), then the attenuation is

$$\frac{\epsilon}{\epsilon_o} = \frac{E(x, t) + 4\pi N e y(t)}{E(x, t)} = 1 + 4\pi N e \left[\frac{y(t)}{E(x, t)} \right], \quad (5.12)$$

where $y(t)$ is the given by Eq. 5.10, and $E(x, t)$ is given by Eq. 5.11. Substituting for $y(t)/E(x, t)$, and solving for the attenuation via Taylor expansion, gives

$$\left(\frac{\epsilon}{\epsilon_o} \right)^{1/2} \simeq 1 + \frac{2\pi N e^2}{m_e} \frac{1}{\omega_o^2 - \omega^2 + i\Gamma\omega}. \quad (5.13)$$

Rewriting Eq. 5.13 in terms of the real and complex parts, $(\epsilon/\epsilon_o)^{1/2} = R + iK$, we have,

$$R = 1 + \frac{2\pi N e^2}{m_e} \frac{\omega_o^2 - \omega^2}{(\omega_o^2 - \omega^2)^2 + \Gamma^2\omega^2} \quad (5.14)$$

and

$$K = \frac{2\pi N e^2}{m_e} \frac{\Gamma\omega}{(\omega_o^2 - \omega^2)^2 + \Gamma^2\omega^2}. \quad (5.15)$$

To obtain the attenuated intensity, $I_\omega(x)$, as function of x through the medium, we compute the complex conjugate of Eq. 5.11, which gives

$$E(x, t)E^*(x, t) \equiv I_\omega(x) = I_\omega^o \exp \left[- \left(\frac{2K\omega}{c} \right) x \right], \quad (5.16)$$

where K (Eq. 5.15) is the complex part of the attenuation term $(\epsilon/\epsilon_o)^{1/2}$. Eq. 5.16 has the form of Eq. 5.8,

$$I_\lambda = I_\lambda^o \exp [-\tau_\lambda], \quad (5.17)$$

with $\omega = 2\pi c/\lambda$. From the definition, $d\tau_\lambda = \ell_\lambda \rho dx$, direct integration gives

$$\tau_\lambda = \ell_\lambda \rho x, \quad (5.18)$$

so that we can write

$$I_\lambda(x) = I_\lambda^o \exp[-\ell_{\lambda\rho}x], \quad (5.19)$$

which is the attenuation as a function of x through the medium (cloud). Direct comparison of Eqs. 5.16 and 5.19 gives $\ell_{\lambda\rho} = 2K\omega/c$. We have

$$\ell_{\lambda\rho} = \frac{2K\omega}{c} \quad (5.20)$$

$$= \frac{4\pi N e^2}{m_e c} \frac{\Gamma \omega^2}{(\omega_o^2 - \omega^2)^2 + \Gamma^2 \omega^2} \quad (5.21)$$

$$= N \frac{\pi e^2}{m_e c} \frac{\Gamma}{(\Delta\omega)^2 + (\Gamma/2)^2}, \quad (5.22)$$

where we have used the approximation $\omega_o^2 - \omega^2 = 2\omega\Delta\omega$, where $\Delta\omega = \omega_o - \omega$, since the function peaks only when $\omega \simeq \omega_o$. This absorption profile is called a “natural”, “damping”, or more formally, a Lorentzian profile.

5.3.1 The Line Absorption Coefficient

We define the natural absorption coefficient per atom, α_{nat} , from

$$\ell_{\lambda\rho} = N\alpha_{nat}(\lambda), \quad (5.23)$$

here we remind that N is the column density of absorbing atoms. Employing $\Delta\omega = -(2\pi c/\lambda_o^2)\Delta\lambda$, and substituting into Eq. 5.22, we can then write α_{nat} in terms of λ as

$$\alpha_{nat}(\lambda) = \frac{e^2}{m_e c} \frac{\lambda_o^2}{c} \frac{\Gamma \lambda_o^2 / 4\pi c}{(\Delta\lambda)^2 + (\Gamma \lambda_o^2 / 4\pi c)^2}, \quad (5.24)$$

The normalization of $\alpha_{nat}(\lambda)$ follows from

$$\int_{-\infty}^{\infty} \frac{\beta}{(x^2 + \beta^2)} dx = \pi. \quad (5.25)$$

Direct integration of the absorption coefficient (Eq. 5.24) over the profile yields

$$\int_0^{\infty} \alpha_{nat}(\lambda) d\lambda = \int_{-\infty}^{\infty} \alpha_{nat}(\Delta\lambda) d\Delta\lambda = \frac{\pi e^2}{m_e c} \frac{\lambda_o^2}{c} \quad (5.26)$$

which is the energy per second per atom per square radian absorbed by a bound-bound transition. This quantifies the rate at which energy is removed from the light beam due to a bound-bound transition with central wavelength λ .

5.3.2 The Damping Constant

In the quantum mechanical treatment of emission, the probability that a photon is emitted in time dt into solid angle $d\Omega$ is

$$A_{ul} dt d\Omega \quad [\text{spontaneous emission}] \quad (5.27)$$

$$B_{ul} I_\lambda dt d\Omega \quad [\text{stimulated emission}]. \quad (5.28)$$

We have introduced the Einstein coefficients for spontaneous and stimulated emission, A_{ul} and B_{ul} , where the subscripts u and l denote the upper and lower energy levels. The Einstein A coefficient has units [Hz radians⁻²]. For stimulated emission, an incident photon stimulates the downward transition; note that the probability is proportional to I_λ , where $\lambda = hc/(E_u - E_l)$ is the wavelength corresponding to the energy difference between the upper and lower energy levels of the bound-bound transition. Thus, the B coefficient has units [erg⁻¹ Hz radians⁻²]. The probability that an incident photon is absorbed in a bound-bound transition can similarly be written

$$B_{lu} I_\lambda dt d\Omega \quad [\text{bound-bound absorption}]. \quad (5.29)$$

Note that the u and l subscripts of B are interchanged.

Consider an equilibrium state of radiative transitions (number of $l \rightarrow u$ is equal to number of $u \rightarrow l$). For a transition from an upper to a given lower energy level, the number of spontaneous emissions per unit second per unit volume is

$$\frac{dn_u}{dt} = -4\pi n_u A_{ul}, \quad (5.30)$$

where n_u is the number density of excited atoms with electrons in the upper level. The rate of stimulated emission per second per unit volume is

$$dn_u/dt = -4\pi n_u B_{ul} I_\lambda, \quad (5.31)$$

where I_λ is taken at the λ of the transition to the lower level. The rate for absorption is similarly written

$$dn_l/dt = -4\pi n_l B_{lu} I_\lambda. \quad (5.32)$$

In equilibrium,

$$n_u A_{ul} + n_u B_{ul} I_\lambda = n_l B_{lu} I_\lambda. \quad (5.33)$$

It follows from the Planck radiation law that

$$B_{ul} = \frac{g_l}{g_u} B_{lu} \quad (5.34)$$

and

$$A_{ul} = 2h\lambda_{ul}^3 B_{ul} = 2h\lambda_{lu}^3 \frac{g_l}{g_u} B_{lu} \quad (5.35)$$

where g_l and g_u are the statistical weights of the lower and upper states, respectively, and clearly, $\lambda_{ul} = \lambda_{lu}$.

Consider spontaneous emission, which is easiest to visualize. From Eq. 5.30, the total downward rate of a bound-bound transition per second per volume from an upper level u is,

$$\frac{dn_u}{dt} = \sum_{l < u} -4\pi n_u A_{ul} = -4\pi n_u \sum_{l < u} A_{ul}, \quad (5.36)$$

where the sums is over all levels lower than the upper level. The solution takes the form

$$n_u(t) = n_u \exp(-t/\Delta t_u), \quad (5.37)$$

where Δt_u is the characteristic time that the electrons spend in the upper level before transitioning downward to some lower level l . Defining $\Gamma_u = 1/\Delta t_u$, we have

$$\Gamma_u = 4\pi \sum_{l < u} A_{ul}, \quad (5.38)$$

which has units of inverse time [Hz]. Therefore, the damping constant Γ_u represents the inverse of the probable time interval that electrons remain in the upper level. Finally, in equilibrium, the absorption damping constant is given by

$$\Gamma_l = 8\pi h \sum_{l < u} \lambda_{lu}^3 \frac{g_l}{g_u} B_{lu}, \quad (5.39)$$

which follows from Eq. 5.35.

In a classical world, the upper, u , and lower, l , energy levels, E_u and E_l , are well defined. However, in reality, there is uncertainty in these energy levels governed by Heisenberg's Uncertainty Principle,

$$\Delta E_u \Delta t_u = h/2\pi \quad \text{and} \quad \Delta E_l \Delta t_l = h/2\pi, \quad (5.40)$$

where ΔE_u and ΔE_l are the uncertainties in the upper and lower energy levels, and Δt_u and Δt_l are the characteristic times that the electron spends in the upper and lower energy levels, respectively. The damping constant and the uncertainty in the energy level are related through

$$\Delta E_u = \frac{h}{2\pi\Gamma_u} = 2h \sum_{l < u} A_{ul}, \quad (5.41)$$

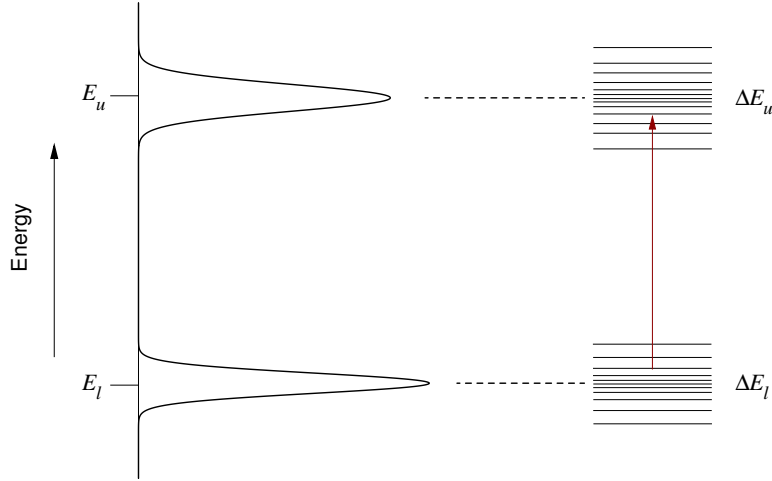


Figure 5.3: — A schematic energy level diagram of a bound-bound transition illustrating the relative spreads in the energies of the upper and lower levels. A transition is shown with the vertical arrow between the two levels. Note that it does not have $E_u - E_l$ precisely, but a slightly offset energy based upon the relative probabilities in both the upper and lower levels.

$$\Delta E_l = \frac{h}{2\pi\Gamma_l} = 4h^2 \sum_{l < u} \lambda_{lu}^3 \frac{g_l}{g_u} B_{lu}. \quad (5.42)$$

Since the bound-bound transitions involves time spent by the electron in both the upper and lower energy levels, we have

$$\Gamma = \Gamma_u + \Gamma_l. \quad (5.43)$$

As illustrated in Fig 5.3, it is the probability distribution of this spread of photon energies due to uncertainty in the energy levels, that results in the shape of the Lorentzian absorption coefficient (Eq. 5.24).

5.3.3 The Oscillator Strength

Actual lab measurements of the energy rate removed by bound-bound transitions often yield *smaller* values than those obtained by the mathematical integration of α_{nat} in Eq. 5.26. Recall that the derivation of the absorption coefficient, α_{nat} , as written in Eq. 5.24, is based upon a classical model of electron interactions with electric fields.

From the quantum mechanical perspective, the integral of Eq.5.26 equates the energy removed from the beam to the probability of a bound-bound

transition $(\lambda^2/c)B_{lu}$ times the energy hc/λ , such that

$$\int_{-\infty}^{\infty} \alpha_{nat}(\lambda) d\Delta\lambda = \frac{hc}{\lambda} \frac{\lambda^2}{c} B_{lu}, \quad (5.44)$$

where B_{lu} is defined in Eq. 5.28. The convention is to introduce into Eq.5.26 a proportionality constant called the oscillator strength, or f value,

$$\int_{-\infty}^{\infty} \alpha_{nat}(\lambda) d\Delta\lambda = \frac{\pi e^2}{m_e c} \frac{\lambda^2}{c} f = \frac{hc}{\lambda} \frac{\lambda^2}{c} B_{lu}, \quad (5.45)$$

where $f < 1$ (though there are rare instances when $f > 1$). Solving for f ,

$$f = \frac{m_e c}{\pi e^2} \frac{hc}{\lambda} B_{lu}, \quad (5.46)$$

5.3.4 Atomic Constants

The transition wavelength, the oscillator strength, and damping constant constitute the atomic constants for each transition. In Table 5.1. the atomic constants are listed for selected transitions that are commonly seen in absorption in quasar spectra.

Table 5.1: Atomic Constants for Selected Transitions

Ion/Tran	λ [Å]	f	Γ [10^8 s^{-1}]
Ly α	1215.670	0.41640	6.265
Ly β	1025.722	0.07912	1.897
O VI λ 1032	1031.927	0.13290	4.163
O VI λ 1038	1037.616	0.06609	4.095
N V λ 1239	1238.821	0.15700	3.411
N V λ 1243	1242.804	0.07823	3.378
Si IV λ 1394	1393.755	0.52800	9.200
Si IV λ 1403	1402.770	0.26200	9.030
C IV λ 1548	1548.195	0.19080	2.654
C IV λ 1551	1550.770	0.09522	2.641
Mg II λ 2796	2796.352	0.6123	2.612
Mg II λ 2803	2803.531	0.3054	2.592

Though oscillator strengths, f , and damping constants, Γ , can be expressed in terms of fundamental quantities, they are measured in the laboratory for each transition and carry an uncertainty of $\sim 10\%$.

From Eq. 5.45, note that the amount of energy removed from the photon beam (in this case the quasar light) scales with $\lambda^2 f$ and has no dependence upon Γ . Thus, the relative magnitude of energy removed from the beam for the well-known doublets listed in Table 5.1 is proportional to the ratio of their $\lambda^2 f$ values. (Note, however that the wavelength difference for doublets is small).

For most doublets, the f values differ by a factor of two between the two transitions. In most all case the bluer transition in a doublet has a larger f value than that of the redder transition, i.e. $f_b = 2f_r$. However, there are rare cases where this is not the case, such as with the Si II $\lambda\lambda 1190, 1193$ doublet, for which $f_r = 2f_b$.

5.4 Thermal Broadening

In reality, absorption lines are always broader than the natural widths described in the above absorption coefficients. In intervening quasar absorption lines, the additional broadening is thermal and/or thermal plus turbulent. Below, we will discuss the thermal broadening function, how it contributes to the observed line profiles and also how the natural and thermal broadening are combined into what is called the Voigt profile.

In an isothermal gas, each atom has an observable radial component of velocity, v_{rad} . Bound-bound transitions in atoms moving toward the observer with velocity, v_{rad} , will absorb photons with wavelengths shorter than the rest-frame transition wavelength, λ_r , by the amount

$$\lambda = \lambda_r \left(1 - \frac{v_{rad}}{c} \right) \quad [\text{toward observer}], \quad (5.47)$$

whereas transitions in atoms moving away from the observer will absorb photons with longer wavelengths by the amount

$$\lambda = \lambda_r \left(1 + \frac{v_{rad}}{c} \right) \quad [\text{toward observer}]. \quad (5.48)$$

These relationships follow from the Doppler shift

$$\frac{\Delta\lambda}{\lambda_r} = \frac{v_{rad}}{c}, \quad (5.49)$$

where $\Delta\lambda = \lambda - \lambda_r$ and for $v_{rad} \ll c$. In terms of the most probable velocity, v_o , for an atom in a gas with temperature T , we obtain the characteristic

Doppler shift,

$$\Delta\lambda_D = \frac{v_o}{c}\lambda_r = \frac{\lambda_r}{c} \left(\frac{2kT}{m} \right)^{1/2}, \quad (5.50)$$

where v_o is taken from Eq. 4.6. Often, $\Delta\lambda_D$ is referred to as the Doppler width. These Doppler shifts modify the observed absorption line profile by spreading the absorption over a wider range of wavelengths. At each radial velocity the absorbing atoms form a natural absorption profile with an amplitude modulated by the number of atoms at that velocity. From Eq. 4.8, the probability that an atom will have velocity v_{rad} is

$$f(v_{rad}) = \frac{1}{\sqrt{\pi}v_o} \exp \left[- \left(\frac{v_{rad}}{v_o} \right)^2 \right] dv_{rad}, \quad (5.51)$$

Substituting the expression for $\Delta\lambda_D$ into Eq. 5.51, we obtain the distribution of $\Delta\lambda$ removed from the beam to be

$$f(\Delta\lambda)d\lambda = \frac{1}{\sqrt{\pi}\Delta\lambda_D} \exp \left[- \left(\frac{\Delta\lambda}{\Delta\lambda_D} \right)^2 \right] d\lambda, \quad (5.52)$$

where

$$\int_{-\infty}^{\infty} f(\Delta\lambda)d\lambda = 1. \quad (5.53)$$

Since $\Delta\lambda_D$ is proportional to the gas temperature, the wavelength spread of the absorption increases with increasing temperature. Also, as temperature increases, the relative amplitude of atoms with $v_{rad} = 0$ decreases, resulting in a flatter distribution of absorption with $\Delta\lambda$.

5.4.1 Redshifted Absorption

In the above discussion of the thermal distribution of atoms it was assumed that the observer was in the rest frame of the absorbing complex. However, the formalism applies in cases where the entire absorbing complex is in motion, as long as there is a velocity zero point in the rest frame of the absorbing complex.

Consider a gas “cloud” with redshift z . Then the observed wavelength at the absorption line center will be $\lambda_{obs} = \lambda_r(1+z)$. In this cloud, consider atoms moving toward the observer with velocity v_{rad} , where v_{rad} is relative to the velocity zero point in the cloud. The observed wavelength will be

$$\lambda = \lambda_{obs} \left(1 - \frac{v_{rad}}{c} \right) = \lambda_r (1+z) \left(1 - \frac{v_{rad}}{c} \right), \quad (5.54)$$

From the Doppler shift formula

$$\frac{\lambda - \lambda_{obs}}{\lambda_{obs}} = \frac{\lambda_r(1+z)(1 - v_{rad}/c) - \lambda_r(1+z)}{\lambda_r(1+z)} = -\frac{v_{rad}}{c}, \quad (5.55)$$

which recovers velocity in the rest frame of the cloud and shows that the Doppler shift formula is invariant with redshift.

The same invariance holds for the distribution of $\Delta\lambda$ removed from the beam due to thermal motions given by Eq. 5.52. The observed Doppler width, $\Delta\lambda_D^{obs}$, will be broadened for a redshifted cloud,

$$\Delta\lambda_D^{obs} = \frac{\lambda_r(1+z)}{c} \left(\frac{2kT}{m} \right)^{1/2} = \Delta\lambda_D(1+z). \quad (5.56)$$

Due to the invariance of the Doppler shift formula, we also have

$$\Delta\lambda_{obs} = \lambda(1+z) - \lambda_r(1+z) = \Delta\lambda(1+z). \quad (5.57)$$

Writing Eq. 5.52 in the redshifted frame,

$$f(\Delta\lambda_{obs})d\lambda_{obs} = \frac{1}{\sqrt{\pi}\Delta\lambda_D^{obs}} \exp \left[- \left(\frac{\Delta\lambda_{obs}}{\Delta\lambda_D^{obs}} \right)^2 \right] d\lambda_{obs}, \quad (5.58)$$

and substituting the redshift explicit terms on the right hand side, gives

$$f(\Delta\lambda_{obs})d\lambda_{obs} = \frac{1}{\sqrt{\pi}\Delta\lambda_D(1+z)} \exp \left[- \left(\frac{\Delta\lambda(1+z)}{\Delta\lambda_D(1+z)} \right)^2 \right] (1+z)d\lambda,$$

and we have

$$f(\Delta\lambda_{obs})d\lambda_{obs} = f(\Delta\lambda)d\lambda. \quad (5.59)$$

Thus, even though the observed broadening of an absorption line is increased when it arises in a redshifted cloud, the distribution of velocities is an invariant quantity. As such, Eq. 5.52 can be universally applied to clouds of all redshifts.

5.5 The Voigt Profile

The Voigt profile gives the distribution of absorption as a function of wavelength when the natural absorption coefficient per atom for natural broadening is modulated by the thermal distribution of atoms. The optical depth, τ_λ , then, takes on the shape of the Voigt profile through the convolution

$$\tau_\lambda = N\alpha(\lambda) = N\alpha_{nat}(\lambda) \otimes f(\Delta\lambda), \quad (5.60)$$

where N is the column density, $\alpha_{nat}(\lambda)$ is the natural absorption coefficient per atom (Lorentzian) given by Eq. 5.24 and $f(\Delta\lambda)$ is the normalized probability distribution of atoms (Gaussian) given in Eq. 5.52. An explicit writing of Eq. 5.60 is

$$\tau_\lambda = \int_{-\infty}^{\infty} N\alpha_{nat}(\lambda')f(\lambda' - \lambda)d\lambda', \quad (5.61)$$

which must be evaluated at each λ to obtain the observed line shape. Expanding gives

$$\tau_\lambda = N \frac{e^2\lambda_r^2}{m_e c^2} f \frac{\Gamma\lambda_r^2/4\pi c}{(\Delta\lambda)^2 + (\Gamma\lambda_r^2/4\pi c)^2} \otimes \frac{1}{\sqrt{\pi}\Delta\lambda_D} e^{-(\Delta\lambda/\Delta\lambda_D)^2}, \quad (5.62)$$

where the transition wavelength, λ_r , has been written explicitly, $\Delta\lambda = \lambda - \lambda_r$, and the f value has been included into the normalization from Eq. 5.45. Note the integral of $\alpha(\lambda)$ is still the energy per second per atom per square radian absorbed by the bound-bound transition, $(\pi e^2/mc)(\lambda^2/c)f$.

The convolution of a Lorentzian and a Gaussian is the Voigt function, u , which has unit normalization. The absorption coefficient with wavelength can be written

$$\tau_\lambda = N \frac{\pi e^2\lambda_r^2}{m_e c^2} f u(x, y) \quad \text{where} \quad u(x, y) = \frac{1}{\sqrt{\pi}\Delta\lambda_D} H(x, y) \quad (5.63)$$

and where the convolution is conveniently expressed by the Hjerting function,

$$H(x, y) = \frac{y}{\pi} \int_{-\infty}^{\infty} \frac{\exp(-t^2)}{(x-t)^2 + y^2} dt \quad (5.64)$$

with

$$x = \frac{\Delta\lambda}{\Delta\lambda_D} \quad \text{and} \quad y = \frac{\Gamma\lambda_r^2}{4\pi c} \frac{1}{\Delta\lambda_D}. \quad (5.65)$$

Note that x acts as the independent variable. It simply is the difference between the wavelength along the profile and the line center in units of the Doppler width. Also note that y is not a function of $\Delta\lambda$ and therefore does not vary with location across the absorption profile. For the given transition, the y is a function of only the damping constant, the wavelength of the line center, and the Doppler width. As seen in Eq. 5.50, the latter depends upon the gas temperature, the wavelength of the line center, and the mass of the atom. Note that the Doppler width also appears in the normalization of the Voigt function, u .

The observed absorption profile will then have the shape

$$I_\lambda = I_\lambda^o \exp[-\tau_\lambda], \quad (5.66)$$

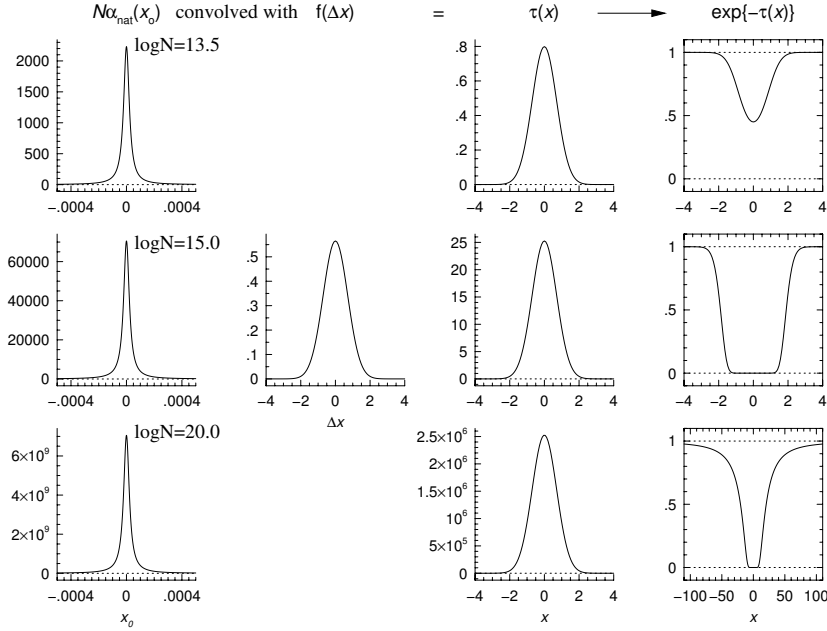


Figure 5.4: — A schematic of the convolution process to obtain the observed line shape in units of $x = \Delta\lambda/\Delta\lambda_D$ for the Ly α transition. The left hand panels are the natural broadening, $N\alpha_{nat}(x)$ for $\log N = 13.5, 15.0,$ and 20.0 [cm^{-2}] from top to bottom. Modulated by the line of sight velocity distribution of atoms (via convolution with Eq. 5.52, which is shown in the second panel from the left), yields the optical depth profile, $\tau(x)$ (second panel from the right). Applying Eq. 5.66 gives the absorption profile. (right hand panels).

where I_λ is the observed flux at wavelength λ and I_λ^o is the quasar continuum flux (in the absence of the absorption line).

An illustration of the convolution process for obtaining Eq. 5.66 is shown in Figure 5.4 for Ly α transitions with $\log N = 13.5, 15.0,$ and 20.0 [cm^{-2}] (from top to bottom). In the left hand panels, the natural profile, $N\alpha_{nat}$, is shown for atoms centered at location x_o . Note the extreme narrowness of the profile, plotted over the range $-0.0005 \leq x_o \leq 0.0005$. The width is governed by $\Gamma\lambda_r^2/4\pi c$, and is independent of $\Delta\lambda_D$. Also note that the natural profile shape is independent of the column density, N , but that the amplitude scales linearly with N . The convolution with Eq. 5.52 ($f(\Delta x)$, second panel from left) modulates for the thermal distribution of atoms (column density) at each x_o , and yields the optical depth, $\tau(x)$. Note that, for the small x ranges shown (near the line centers) the $\tau(x)$ profile shapes emulate the shape of $f(\Delta x)$ and are independent of N . This is because

the natural widths are extremely narrow. However, the amplitudes vary by orders of magnitude depending upon N . For the $\log N = 13.5 \text{ cm}^{-2}$ case, $\tau(x) < 1$ for all x . At each x_o , the atoms at x_o generate an $N\alpha_{nat}$ profile with amplitude modulated by $f(\Delta x)$.

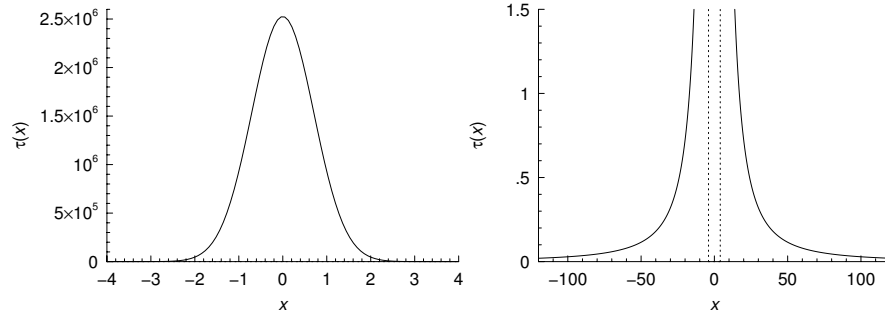


Figure 5.5: — (left) The optical depth, $\tau(x)$, reproduced from Fig 5.4 for the $\log N = 20.0 \text{ cm}^{-2}$ case over the range $-4 \leq x \leq 4$. — (right) The same $\tau(x)$ profile in an expanded view. Note how the wings of the optical depth emulate those of the natural broadening, $N\alpha(x)$, giving rise to the so-called damping wings in the observed absorption profile (shown in the bottom right panel of Fig 5.4). Vertical dashed lines mark the x range shown in the left panel.

The right hand panels of Figure 5.4 are the observed line profiles as given by Eq. 5.66. Note that when the optical depth is less than unity, the absorption line profile is not black (upper right panel), but that for $\tau(x) \gg 1$, the absorption becomes black. For the $\log N = 20.0 \text{ cm}^{-2}$ example, the x scale is greatly expanded by a factor of ~ 30 ! This is to show the so-called damping wings. For large x , the $\tau(x)$ profile emulates the wings of $N\alpha_{nat}$ profile. An expanded scale of the $\tau(x)$ for $\log N = 20.0 \text{ cm}^{-2}$ is shown in Fig 5.5. Note that the optical depth remains greater than unity to $x \pm 20$ and decreased very slowly with increasing x .

Profiles such as those shown in the right hand panels of Figure 5.4 can be fit to Eq. 5.66 to objectively obtain the column density, N , and the only additional free parameter, the Doppler width, $\Delta\lambda_D$. This approach is useful only for high resolution data in which the line width induced by the instrument (see § 7.1.6) is significantly less than the Doppler width. Usually the fitting of the data is performed using the technique of χ^2 minimization (§ 3.6). In high resolution spectra, the absorption lines often break up into multiple components, forming a complex and often blended profile shape. We will address this further complexity in Chapter 8.2.

5.6 The Doppler b Parameter

In practice, the Doppler widths are written as the Doppler b parameter,

$$b = \frac{c}{\lambda} \Delta\lambda_D = \left(\frac{2kT}{m_i} \right)^{1/2}, \quad (5.67)$$

where m_i is the mass of the atom in which the transition arises (and not the electron mass). Substituting into Eq. 5.65, we have

$$x = \frac{v_{rad}}{b} \quad \text{and} \quad y = \frac{\Gamma\lambda_r}{4\pi b}, \quad (5.68)$$

where $v_{rad}/c = \Delta\lambda/\lambda_r$. Substituting into Eq. 5.62, and rearranging yields,

$$\tau(v_{rad}) = N \frac{e^2}{m_e b} f \frac{y}{x^2 + y^2} \otimes \frac{1}{\sqrt{\pi} b} e^{-x^2}, \quad (5.69)$$

where

$$\tau(v_{rad}) = N \frac{\pi e^2}{m_e b} f u(x, y) \quad \text{where} \quad u(x, y) = \frac{1}{\sqrt{\pi} b} H(x, y), \quad (5.70)$$

and where $H(x, y)$ is given by Eq. 5.64. This form of the absorption coefficient is useful for measuring the individual velocity components of complex absorption profiles (see § 8.2.7). The conversion between λ in the rest-frame and v_{rad} is simply given by the Doppler shift formula (Eq. 5.49),

$$v_{rad} = c \frac{\lambda - \lambda_r}{\lambda_r} \quad (5.71)$$

If the absorption line is observed at redshift z , then the conversion between λ in the observer frame and v_{rad} in the rest frame is

$$v_{rad} = c \frac{\lambda - \lambda_r(1+z)}{\lambda_r(1+z)} \quad (5.72)$$

Given an observed redshifted absorption profile with multiple components, the goal is to objectively determine the velocities (i.e., redshifts) in addition to the column densities and Doppler b parameters of each component. As mentioned above, this usually involves the χ^2 minimization technique (§ 3.6). We will address Voigt profile fitting of the data in § 8.2.7.

5.6.1 Turbulent Broadening

If two absorption lines arise in the same isothermal gas cloud, one from an atom with mass m_1 and the other with m_2 , then the ratio of their b parameters would be $b_1/b_2 = (m_2/m_1)^{1/2}$. If $m_1 > m_2$, then $b_1 < b_2$. The heavier atom has a smaller b . If there is turbulence in the gas, then the above mass dependence between different atoms will break down.

Turbulence acts as another source of line broadening. Unfortunately, it is not clear how to describe the broadening function. First, the turbulent component to the broadening function would require unit normalization and would need to be convolved with the absorption coefficient as written in Eqs. 5.62.

A simple functional form for turbulent motion is a Gaussian. Though this is somewhat unphysical, it has the merit of preserving the Voigt function formalism of the total absorption coefficient. The convolution of two Gaussian functions, one having having dispersion σ_a and the second having σ_b is a Gaussian having

$$\sigma_c^2 = \sigma_a^2 + \sigma_b^2. \quad (5.73)$$

Thus, the Gaussian component appearing in Eq. 5.62 can be written such that the Doppler widths $\Delta\lambda_D$ and $\Delta\nu_D$ are replaced with

$$b^2 = b_{therm}^2 + b_{turb}^2 = \frac{2kT}{m} + b_{turb}^2, \quad (5.74)$$

where the notation is given as Doppler b parameters.

Note that the thermal component is dependent upon the mass of the atom, whereas the turbulent component is independent of mass. If, in a given gas cloud, $b_{turb} \gg b_{therm}$, then all absorption lines will have the same measured b .

In the more general case, when neither the thermal nor the turbulent component dominate, it is possible to deconvolve b_{tot} when transitions from at least two different atoms have been observed. We have

$$b_1^2 = \frac{2kT}{m_1} + b_{turb}^2 \quad \text{and} \quad b_2^2 = \frac{2kT}{m_2} + b_{turb}^2, \quad (5.75)$$

from which we obtain

$$b_{1,therm}^2 = \frac{b_1^2 - b_2^2}{1 - (m_1/m_2)} \quad (5.76)$$

where the temperature is found from $T = (m_1/2k)b_{1,therm}^2$. Solving for the turbulent component yields,

$$b_{turb}^2 = \frac{b_2^2 - (m_1/m_2)b_1^2}{1 - (m_1/m_2)}. \quad (5.77)$$

When transitions from more than two atoms are present, additional constraints can be placed on the cloud temperature and the relative contribution of the turbulent b component. Note that the method is most powerful for large mass ratios.

